Eye-safety analysis of current laser-based LCOS projection systems

Edward Buckley (SID Member)

Abstract — A laser safety analysis for liquid-crystal–on–silicon (LCOS) based imaging projection systems utilizing laser light sources is presented. It is shown that a typical laser-based imaging projector is capable of providing a D65 white-balanced luminous flux in excess of 20 lm while remaining Class 1 eye safe. By considering a Class 2 classification, it is shown that the same architecture is capable of providing several hundred lumens, a performance level which could potentially be applicable to a new class of high-brightness miniature projection systems.

Keywords — *Laser, safety, LCOS, projection.*

DOI # 10.1889/JSID18.12.1051

1 Introduction

Miniature projection systems based on LEDs emerged in 2008, and the resultant "pico-projector" products, typically providing luminous flux of less than 10 lm, have enjoyed significant and increasing market penetration.[1] The successful pico-projector products to date have utilized LED-illuminated imaging technologies, *i.e.*, the optical system utilizes an amplitude-modulating microdisplay, which is illuminated with white light in the case of color-filter panels[2,3] or color sequentially in the case of fast nematic[4] or ferroelectric[5] liquid-crystal–on–silicon (LCOS) panels.

LCOS-based systems utilizing laser illumination will, in the future, provide a smaller form factor, longer depth of field, polarization independence, and potentially higher efficiencies once concerns regarding speckle and current supply-chain restrictions are alleviated. The first consumer pico-projector products featuring a laser-based LCOS light engine[6] were introduced in 2010, and non-imaging holographic projection systems employing a phase-modulating LCOS panel[7] hold further significant promise. It is widely anticipated that laser-based light engines will soon exceed the performance demonstrated by current LED-based counterparts, and some very encouraging recent progress[8] has given credence to these expectations.

Yet, despite the much-vaunted advantages of the combination of laser illumination and widely available LCOS imaging microdisplays – especially the extended color gamut and potential for higher perceived brightness as a result of the Helmholtz–Kohlrausch effect[9] – the extent to which the brightness of such systems can increase while maintaining an acceptable laser safety classification is still widely misunderstood. This is likely to become an increasingly important issue as these systems move towards commoditization, possibly by integration into devices such as cellphones.

In this paper, a model consistent with the European laser safety standard IEC 60825-1 (which is being adopted by the U.S. in changes to the Federal Standard[10,11]) is used to derive the output power restrictions imposed by Class 1 and Class 2 laser safety classes upon imaging projection displays systems and, as in previous studies,[12] the corresponding D65 resultant white-balanced luminous flux values.

2 Analysis methodology

Lasers are classified by wavelength and maximum output power into four classes according to their ability to produce damage in exposed people, from Class 1 (which represents no hazard during normal use) to Class 4 (severe hazard for eyes and skin). A given laser safety classification is defined by an Acceptable Exposure Limit (AEL), which is dependent upon a number of physiological and technology-specific factors and is expressed as a maximum power in Watts (W) or energy in Joules (J) that can be emitted in an exposure time at a given wavelength.

As stated by IEC 60825-1,[13] the acceptable exposure limit for visible wavelength laser safety classification is determined by measuring in a limiting aperture of radius d = 7 mm, representative of the maximum dilation of the human eye, at a distance of r = 100 mm from the projection aperture. The measurement geometry is shown in Fig. 1.

Assuming that the power delivered to this aperture is measured over a classification period T_2, the maximum per-

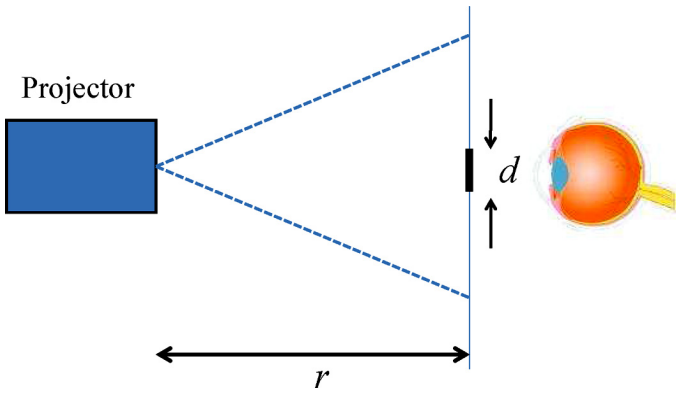

FIGURE 1 — Measurement geometry for determination of the laser safety classification.

Received 07-12-10; accepted 10-23-10.

The author can be reached at P.O. Box 7483, Jackson, WY 83002; telephone 719/271-3939, e-mail: ebuckley@ieee.org.

TABLE 1 — Eye-safety parameters defined by IEC 60825-1.

Quantity	Symbol	Value	Source
Measurement aperture diameter/mm	d	7	Ref. 13, p. 34, Table 10
Measurement aperture distance from source/mm	r	100	Ref. 13, p. 34, Table 10
Minimum source angular subtense/mrad	α_{min}	1.5	Ref. 13, p. 34, Table 10
Maximum source angular subtense/mrad	α_{max}	100	Ref. 13, p. 35, 9.3(*ii*)
Aperture acceptance angle/rad	γ	0.07	Eq. (1)

missible optical power in the measurement aperture that a given laser safety standard allows is determined. By then inferring the total projected image power P_{image}, which would result in this condition and imposing a white-point condition, a photometric measure of maximum luminous flux L_{max} can be derived.

2.1 Projection geometry

A projection system with horizontal and vertical projection angles of θ_h and θ_v radians respectively gives rise to a rectilinear image containing the measurement aperture of diameter d, which is defined to have an acceptance angle γ radians. The side and top views of the projection geometry are illustrated in Fig. 2.

The acceptance angle γ is related to the measurement aperture diameter d and measurement distance r by

$$\tan\left(\frac{\gamma}{2}\right)=\frac{d}{2r}. \tag{1}$$

2.2 General methodology

As previously noted, a given laser safety classification is defined by the AEL. The AEL is strongly influenced by the apparent source size, subtending an angle between α_{min} and α_{max} radians which, in an imaging system, is either set by the size of the microdisplay or the properties of any speckle-reducing diffusing elements. The AEL also depends upon an energy scaling factor pertaining to thermal retina damage, which in turn is weighted by the number and duration of modulated optical pulses delivered to the measurement aperture, and an exposure time t or classification time T_2.

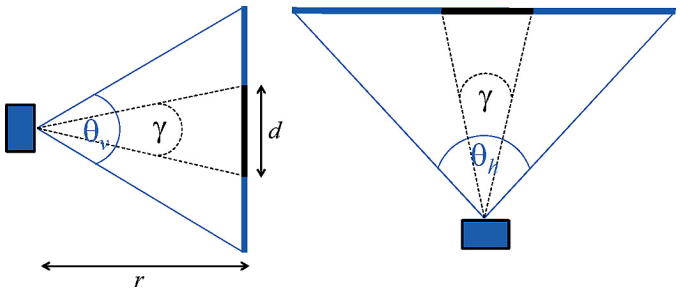

FIGURE 2 — Projection geometry for an image of extent $\theta_h \times \theta_v$ radians, containing the measurement aperture of diameter d and acceptance angle γ.

The generic eye safety parameters defined by IEC 60825-1 are given in Table 1.

In general, there may be several AELs covering single-pulse or pulse-train conditions and photothermal or photochemical effects, so the limiting AEL (measured in Joules, J) is defined as the most restrictive of AEL_n, where $n = 1 \ldots N$, so that

$$AEL(J)=\min\{AEL_1, AEL_2, \ldots, AEL_N\}. \tag{2}$$

The maximum power that can be delivered to the projected image P_{image} is then determined such that the energy at the measurement aperture $E_{aperture}$ is less than the AEL, thereby satisfying

$$E_{aperture} < AEL(J). \tag{3}$$

To calculate the maximum optical image power P_{image} that can be delivered whilst maintaining the appropriate AEL at the measurement aperture, the proportion of energy η delivered to the aperture in T_2 sec is calculated so that

$$E_{aperture} < T_2 \eta P_{image}, \tag{4}$$

where, neglecting any distortion in the image, the fraction of power delivered into the measurement aperture is given to a first-order approximation by

$$\eta \approx \frac{\gamma^2}{\theta_h \theta_v}. \tag{5}$$

As previously shown,[14] panel-based imaging projectors modulate light by selectively blocking and hence the worst-case situation for eye safety corresponds to the full white screen condition. Using this fact and combining Eqs. (3) and (4) gives the result that the radiometric power P_{image} exiting the projection lens should not exceed a limit defined by

$$P_{image} < \frac{AEL(J)}{T_2 \eta} \tag{6}$$

in order to satisfy a given laser safety classification.

3 Imaging projector analysis

In an imaging projector illuminated by laser light, a LCOS panel is used to color-sequentially amplitude modulate the incident illumination. Since the pixel definition is provided directly by the panel pixellation, the modulation frequency

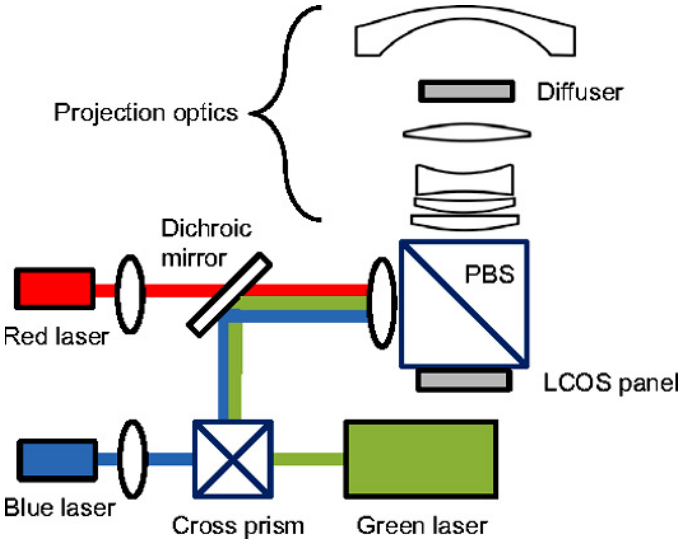

FIGURE 3 — Schematic of example laser projector architecture.[18,19]

required of the lasers is low and is proportional to the frame rate. A relay lens assembly is used to expand the resultant image, and despeckling can be achieved by the use of a diffusing element prior to the final lens of the projection telescope. It is assumed that a D65 white point at a color temperature of 6500K is to be obtained from RGB laser sources of wavelengths λ_b = 445 nm, λ_g = 532 nm, and λ_r = 642 nm such as those manufactured by Nichia,[15] Corning,[16] and Opnext,[17] respectively. A schematic of an example projector architecture is shown in Fig. 3.[18,19]

A ray trace for the diffuser and final lens element is shown in Fig. 4. The presence of the diffuser at the back focal plane of the projection lens causes a beam waist of size w at the front focal plane so that the angular subtense of the source α is given by $\alpha \cong w/r$. If the diffuser has a scattering angle of θ and the projection lens has diameter x, then the angular subtense of the source in terms of the projection lens focal length f is

$$\alpha = \frac{2f}{r}\tan\left(\frac{\theta}{2}\right) \tag{7}$$

by inspection of Fig. 4. Assuming a relatively fast $f/2$ projection lens, as used in current LED-based pico-projector architectures[19] with x = 7 mm, gives f = 15 mm. An

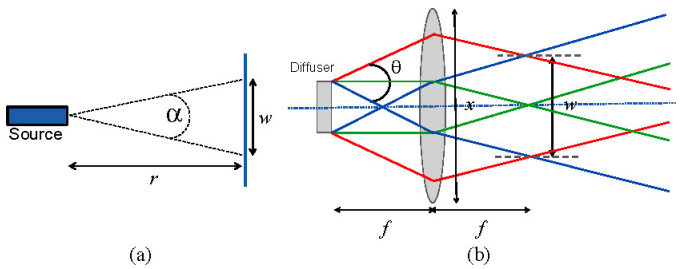

FIGURE 4 — Beam waist w for source of angular subtense α, where r has the same meaning as in Fig. 1(a) and ray trace (b) of an imaging system in which a diffuser of scattering angle θ, present at the back focal plane of a projection lens of focal length f, forms a waist w in the front plane of the projection lens of diameter x.

engineered diffuser with scattering angle of θ = 15° provides an acceptable balance between optical efficiency and speckle reduction[20,21] and this results in a source angular subtense of 40 mrad.

If the projection system has a diagonal throw ratio r_t and forms an image with aspect ratio r_a, then the horizontal and vertical projection angles θ_h and θ_v are given by

$$\tan\frac{\theta_h}{2} = \frac{r_t}{2\sqrt{r_a^2+1}}, \qquad \tan\frac{\theta_v}{2} = \frac{r_a r_t}{2\sqrt{r_a^2+1}}. \tag{8}$$

Current laser-based imaging pico-projectors operate at a diagonal throw ratio r_t = 0.77,[22] providing horizontal and vertical throw angles of θ_h = 37° and θ_v = 21°, respectively, assuming an aspect ratio of 16:9.

Miniature, high-resolution, LCOS displays in this aspect ratio are available from Syndiant[23] and Micron.[24] While the technological approaches are radically different – the former employing a fast nematic material with single-pulse digital drive, and the latter using a fast ferroelectric LC with pulse width modulation (PWM) drive – both are capable of frame rates in excess of f_r = 360 Hz, enabling the minimization of color-breakup artifacts. Recently, materials and drive schemes enabling bistable ferroelectric LCOS microdisplays have been demonstrated,[25] thereby removing the requirement for frame-inversion and enabling a doubling of optical efficiency to match the performance of current nematic liquid-crystal (LC) materials.

A typical drive scheme for a LCOS pixel is shown in Fig. 5. The achievable light throughput is determined by the illumination duty cycle $D < 1$ which, in turn, is related to the blanking time τ_b and delay time τ_d in switching from optical on to off states. Duty cycles of 85%[4] and 89%[25] have been reported in the literature for fast-switching nematic using single-pulse digital drive and bistable ferroelectric LC using DC-balanced PWM drive schemes, respectively.

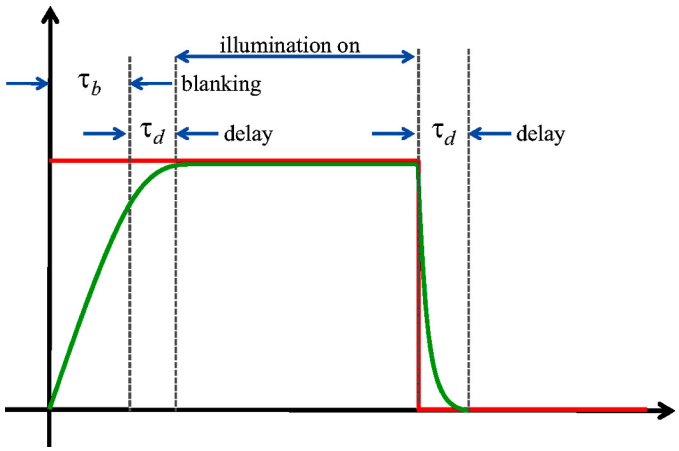

FIGURE 5 — LCOS panel drive waveform (red) and LC response (green), after,[4,25] illustrating blanking time τ_b and delay time τ_d.

TABLE 2 — Summary of the system parameters for a LCOS imaging projection system.

Quantity	Symbol	Value	Source
Aspect ratio	r_a	16:9	
Refresh rate/Hz	f_r	360	Ref. 4
Diagonal throw ratio	r_t	0.77	Ref. 22
Horizontal throw angle/rad	θ_h	0.52	Eq. (8)
Vertical throw angle/rad	θ_v	0.29	Eq. (8)
Projection lens speed		$f/2$	Refs. 26 and 27
Projection lens diameter/mm	x	7	Ref. 4
Projection lens focal length/mm	f	15	
Diffuser scatter angle/deg	θ	15	Ref. 21
Angular subtense of source/mrad	α	40	Eq. (7)
Illumination duty cycle	D	0.85	Refs. 4 and 25

The system-specific parameters presented in this section, both assumed and calculated, are summarized in Table 2.

The aim of the analysis is obtain a maximum luminous flux value for the given laser safety classification. This is achieved by converting the radiometric figure P_{image} for the total output of Eq. (11) into the equivalent photometric quantities at red, green, and blue wavelengths P_r, P_g, and P_g assuming a D65 white balance. The method has been covered previously[12] and will not be repeated here.

3.1 Class 2 operation analysis

The IEC 60825-1 standard defines the Class 2 AEL for an exposure time t, where 1.8×10^{-5} sec $\le t \le 10$ sec and wavelength λ, where 400 nm $\le \lambda \le$ 700 nm, as

$$AEL = 7\times10^{-4} C_6 t^{0.75} \text{ J}, \tag{9}$$

where C_6 is the effective source size correction factor given by

$$C_6 = \begin{cases} 1 & \alpha \le \alpha_{\min} \\ \alpha/\alpha_{\min} & \alpha_{\min} \le \alpha \le \alpha_{\max} \\ \alpha_{\max}/\alpha_{\min} & \alpha < \alpha_{\max} \end{cases} \tag{10}$$

and α is the angular subtense of the source defined in Eq. (7). The beam correction factor assuming a diffuser angle of 15° is found to be C_6 = 26.3. The upper limit, regardless of diffuser strength, is C_6 = 66.7.

3.1.1 Single-pulse analysis

For a single pulse in the visible region, the maximum permissible Class 2 power is given by power is equal to the AEL of Eq. (9) divided by the pulse duration T_i, or

$$AEL_1 = 7\times10^{-4} C_6 T_i^{-0.25} \text{ W}. \tag{11}$$

Using the frame rate f_r = 360 Hz with a duty cycle of 85% results in P_{image} = 4.1 W, using Eq. (5) to account for the fractional aperture area.

3.1.2 Pulse-train analysis

In an imaging projection system, the pulse patterns may be non-uniform depending upon the drive scheme of the LCOS panel in response to variations of scene brightness. For example, ferroelectric displays provide digital gray scale by employing a PWM pixel drive with either equal or monotonically increasing intervals,[5] while nematic panels can employ single-pulse drive. IEC 60825-1 provides a convenient method for treating pulse waveforms in which the individual pulse-to-pulse energies and subpulse structure may vary, but the pulse interval is constant. This is known as the total on-time-pulse (TOTP) method, whereby the AEL is determined by the sum of all pulse durations within the emission duration T_2.[11] By setting $t = nT_i$ for the total pulse on-time in Eq. (11), where n is the number of pulses incident upon the measurement aperture during T_2, the following expression for the Class 2 pulse-train AEL is obtained:

$$AEL = 7\times10^{-4} C_6 \frac{(nT_i)^{0.75}}{T_2} \text{ W}. \tag{12}$$

from which the radiometric image limit P_{image} = 1.1 W follows, equivalent to a D65 white-balanced luminous flux of approximately 281 lm. A summary of the relevant parameter values for the Class 2 safety analysis is provided in Table 3.

3.2 Class 1 operation analysis

For Class 1 operation, the exposure time is defined to be t = 100 sec for 400 ≤ λ ≤ 700 nm and a source of angular extent greater than 1.5 mrad.[13] In the wavelength range

TABLE 3 — Summary of relevant parameter values for the Class 2 safety analysis.

Quantity	Symbol	Value	Source
Blink response classification time/sec	T_2	0.25	Ref. 13, p. 30, 8.4(e) condition (i)
Source size correction factor	C_6	26.3	Ref. 13, p. 39, Table 4 and Eq. (10)
No. pulses incident upon measurement aperture	n	90	
Acceptable exposure limit/mW	AEL	23.1	Ref. 13, p. 36, Table 2 and Eq. (10)
Maximum radiometric power at aperture/mW	P_{image}	1,137	Eqs. (6) and (11)
Maximum luminous flux at aperture/lm	L_{max}	281	Ref. 12

$400 \le \lambda \le 1400$ nm, the classification period T_2 is then defined as

$$T_2(s) = \begin{cases} 10 & \alpha < 1.5 \text{ mrad} \\ 10 \times 10^{\left\lfloor \frac{\alpha - \alpha_{\min}}{98.5} \right\rfloor} & 1.5 \text{ mrad} < \alpha < 100 \text{ mrad} \\ 100 & \alpha > 100 \text{ mrad} \end{cases} \quad (13)$$

which, using the system parameters of Table 2, gives $T_2 \approx 24$ sec. This is much longer than the classification period of $T_2 = 0.25$ sec, chosen to match the human blink reflex, that is used for the equivalent Class 2 standard.

In addition to photothermal limits, the Class 1 classification procedure asserts photochemical power limits for the green and blue wavelengths λ_g and λ_b by including the weighting function C_3, where

$$C_3(\lambda) = 10^{0.02(\lambda - 450)} \quad (14)$$

for $400 \le \lambda \le 700$ nm. To determine a radiometric power figure that satisfies the Class 1 classification requires that the photochemical power at the output of the projector for blue and green wavelengths, and the photothermal power summed across all wavelengths, are less than the respective limits. Expressed mathematically, if the photochemical limits at blue and green wavelengths are $P_{ph}(\lambda_b)$ and $P_{ph}(\lambda_g)$, respectively, and the photothermal output power limit is P_{th}, then to achieve a Class 1 the following must simultaneously hold:

$$\begin{aligned} P_b &< P_{ph}(\lambda_b), \\ P_g &< P_{ph}(\lambda_g), \end{aligned} \quad (15)$$

and

$$P_{image} < P_{th}. \quad (16)$$

3.2.1 Photothermal hazard

For a source of angular subtense $\alpha > 1.5$ mrad, there are two formulae for the AEL depending upon the classification and emission duration T_2 and t, respectively:

$$AEL = \begin{cases} 7 \times 10^{-4} C_6 T_2^{-0.25} \text{ (W)} & t > T_2 \\ 7 \times 10^{-4} C_6 t^{-0.25} \text{ (W)} & t \le T_2 \end{cases}. \quad (17)$$

For continuous-wave (CW) emission, $t = 100$ sec and $T_2 \approx 24$ sec so the first of these conditions apply and the radiometric photothermal power limit is $P_{th} = 5.3$ W. For single-pulse and pulse-train conditions, however, the photothermal AEL is determined by $t = T_i < T_2$ and the second condition is used; $T_i = D/f_r$ in this case, where D is the pulse duty cycle defined by the LC blanking and delay times. For the pulsed mode of operation, it is also necessary to account for the presence of n pulses in the classification duration T_2 by multiplying the AEL by $n^{-0.25}$,[13] so that the final expression for the AEL becomes

$$AEL = 7 \times 10^{-4} C_6 (nt)^{-0.25} \text{ W} \quad (18)$$

from which the approximate radiometric power limit for pulsed operation is found to be $P_{th} = 208$ mW.

3.2.2 Photochemical hazard

The AEL for the photochemical hazard for $t = 100$ sec and a source angular subtense of $\alpha = 11$ mrad is given by

$$AEL(\lambda_b, \lambda_g) = 3.9 \times 10^{-3} C_3(\lambda_b, \lambda_g) \text{ J} \quad (19)$$

which, for $\alpha \ne 11$ mrad, gives a CW photochemical power limit of

$$P_{ph}(\lambda_b, \lambda_g) = \left(\frac{\alpha}{11}\right)^2 \frac{AEL(\lambda_b, \lambda_g)}{\eta t} \text{ W} \quad (20)$$

in the 7-mm measurement aperture. For the photothermal hazard, the thermal contribution of the pulsed waveform was accounted for by applying the "$n^{-0.25}$ rule" to the AEL. This rule is not appropriate for the photochemical hazard and, instead, the power limit of Eq. (20) is reduced according to the duty cycle D so that

TABLE 4 — Summary of the relevant parameter values for the Class 1 safety analysis.

Quantity	Symbol	Value	Source
Emission duration/sec	t	100	Ref. 13, p. 30, 8.4(e) condition (ii)
Photochemical wavelength correction factor	$C_3(\lambda)$	$\lambda = 445$, $C_3 \approx 1$	Ref. 13, p. 39, Table 4
		$\lambda = 532$, $C_3 \approx 44$	
Classification period/sec	T_2	24	Ref. 13, p. 39, Table 4, Eq. (13)
Angle of acceptance/mrad	γ	11	Ref. 13, p. 34, 9.3(c)
No. pulses in T_2 sec	n	8751	
Photochemical power limit at aperture/mW	P_g	919	Eq. (21)
	P_b	16.7	
Photothermal power limit at aperture/mW	P_{th}	208	Eq. (20)
Maximum radiometric power at aperture/mW	P_{image}	62.0	Eqs. (6), (15), and (16)
Maximum luminous flux at aperture/lm	L_{image}	21.0	Ref. 12

$$P_{ph}(\lambda_b,\lambda_g)=\left(\frac{\alpha}{11}\right)^2 AEL(\lambda_b,\lambda_g)\frac{D}{\eta t}\ \text{W}. \qquad (21)$$

For the green and blue wavelengths, respectively, the Class 1 photochemical power limits for pulsed operation are approximately $P_{ph}(\lambda_g)$ = 919 mW and $P_{ph}(\lambda_b)$ = 17 mW.

It is clear that the limiting AEL is determined by the photochemical hazard at the blue wavelength λ_b and hence an iterative method was used to find the radiometric image power limit that satisfied Eqs. (15) and (16) in the pulse-train mode of operation representative of a color-sequential LCOS-based system. The resultant maximum image power corresponding to P_b = 17 mW is P_{image} = 62 mW which corresponds to a D65 white-balanced luminous flux of L_{max} = 21 lm.

A summary of the results and relevant simulation parameters for the Class 1 analysis are summarized in Table 4.

4 Conclusions

A rigorous laser safety analysis was performed for a laser-illuminated imaging system employing a LCOS panel and despeckling diffuser. The maximum achievable D65 white-balanced luminous flux is strongly dependent upon the scattering angle θ of the internal diffuser, and for typical scattering angles of θ = 15°, it was found that an LCOS-based imaging system with λ_b = 445 nm, λ_g = 532 nm and λ_r = 642 nm is limited to approximately 21 lm while maintaining a Class 1 classification and 280 lm for Class 2 – independent of resolution.

For a Class 1 system, the maximum achievable luminous flux can be increased either by increasing the diffuser scatter angle, which could negatively impact optical efficiency, or by increasing the blue laser wavelength λ_b to obtain a concomitantly higher luminous efficacy at the expense of reduced color gamut. Similarly, a shorter red wavelength λ_r could enable a higher luminous flux output while maintaining a Class 2 classification, because the higher luminous efficacy of sources at shorter red wavelengths gives a higher photometric power for the same radiometric power.

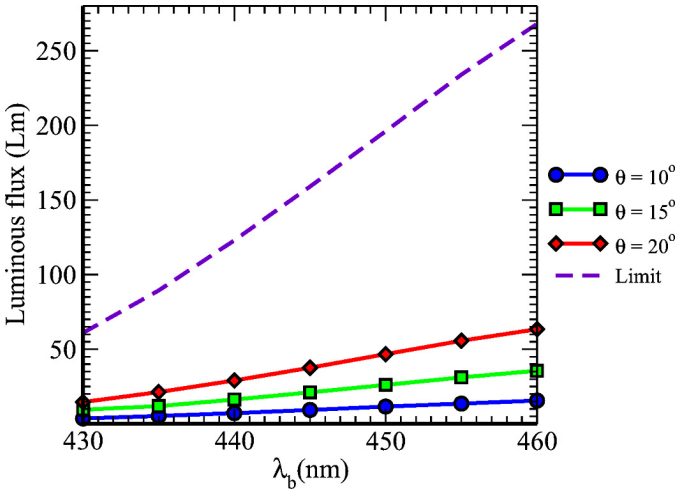

FIGURE 6 — Maximum Class 1 luminous flux as a function of diffuser scatter angle θ and blue laser wavelength λ_b. The dashed line shows the theoretical maximum, corresponding to $\alpha = \alpha_{max}$.

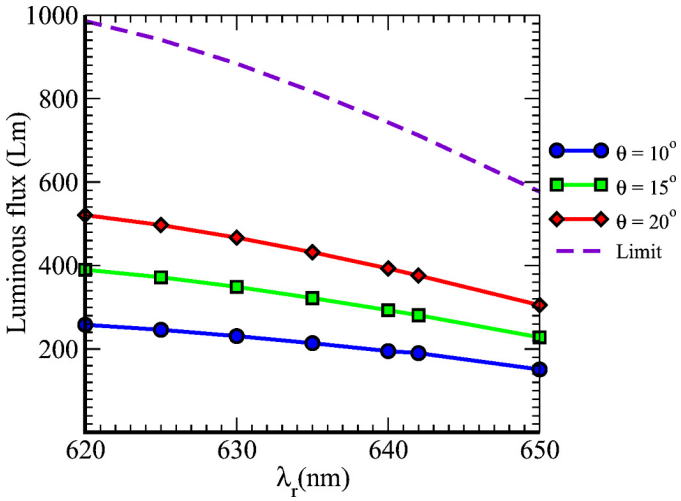

FIGURE 7 — Maximum Class 2 luminous flux as a function of diffuser scatter angle θ and red laser wavelength λ_r. The theoretical maximum, corresponding to $\alpha = \alpha_{max}$, is shown by the dashed line.

Figures 6 and 7 illustrate these points by plotting the maximum achievable luminous flux for Class 1 (a) and Class 2 (b) systems as a function of λ_r and λ_b for diffuser scatter angles of 10°, 15°, and 20°. The theoretical maximum luminous flux for each class, which corresponds to diffuser scatter angles for which $\alpha = \alpha_{max}$, is also indicated.

In conclusion, it can be seen that LCOS-based imaging systems possess a fundamental advantage in terms of laser safety classification compared to scanned-beam projection systems. As shown in this paper, a panel-based pico-projector could achieve a Class 1 laser safety rating while providing a luminous flux of 20 lm independent of resolution. Using the same laser sources, a scanned-beam system, as previously shown,[12] would be limited to between 11 and 15 lm for Class 2 operation and just 1 lm for Class 1 classification.

Since panel-based systems employing laser illumination can now provide the advantages of scanned-beam systems – namely, small size, an efficient optical architecture, long depth of field and a wide color gamut – yet can deliver greater luminous flux while remaining Class 1 eye-safe, panel-based systems could become the dominant technology for greater than 10–20-lm pico-projection applications. In addition, the ability of panel-based systems to deliver several hundred lumens while remaining Class 2 eye-safe could result in the emergence of a new class of high-brightness portable projector.

Using typical optical efficiency figures from an LED pico-projector[19] as a guide, a laser-based projector using an LCOS panel should be able to achieve an 85% illumination duty cycle, 94% temporal fill-factor, 44% optical system efficiency, 91% panel fill-factor, and 80% color-combiner efficiency. Losses due to polarization can be neglected. This leads to a total system throughput efficiency of 26%, requir-

ing red, green, and blue laser powers of approximately 2.2, 1.3, and 0.9 W to produce a luminous flux of 280 lm. Assuming relatively conservative conversion efficiencies of 15%, 10%, and 20% for the red, green, and blue sources, respectively, results in a power consumption on the order of 33 W. Therefore, with the advent of multiple-emitter and multimode laser sources providing several watts per color, a new class of ultra-portable pocket projector, capable of delivering a Class 2 eye-safe luminous flux of 280 lm while consuming less than 40 W, could emerge in the near future.

References

1 Instat LLC, *Embedded Picoprojectors Ready to Break Out Worldwide* (April 2009).
2 H. C. Huang *et al.*, "Color filter liquid-crystal-on-silicon microdisplays," *SID Symposium Digest* **36**, 880–883 (2005).
3 B. L. Zhang *et al.*, "Optical analysis of vertical aligned mode on color filter liquid-crystal-on-silicon microdisplay," *SID Symposium Digest* **37**, 1435–1438 (2006).
4 K. Guttag *et al.*, "854 × 600 pixel LCOS microdisplay with 5.4 μm pixel pitch for pico-projectors," in *Proc. IDW '08* (2008).
5 M. A. Handschy and J. Dallas, "Scalable sequential-color display without asics," *SID Symposium Digest* **38**, 109–112 (2007).
6 Aaxa technologies, "Press release," February 2010. [Online]. Available: http://www.aaxatech.com/news/l1_laser_pico_projector.html.
7 E. Buckley, "Holographic laser projection," *J. Display Technol.* **6**, No. 99, 1–6 (June 2010).
8 Explay, Ltd., "Product specifications," 2010. [Online]. Available: http://www.explay.co.jp/en/products/specs.html.
9 Y. Nayatani, "Relations between the two kinds of representation methods in Helmholtz-Kohlrausch effect," *Color Res. Appl.* **23**, 288–301 (1998).
10 K. Barat and J. E. Dennis, "Laser safety standards through the years," *Photonics Spectra* (June 2010).
11 A. R. Henderson and K. Schulmeister, *Laser Safety* (Taylor and Francis Group, LLC, 2004).
12 E. Buckley, "Eye safety analysis of current laser-based scanned-beam projection systems," *J. Soc. Info. Display* **18**, No. 11, 944–951 (2010).
13 *Safety of laser products – Part 1: Equipment classification, requirements and user's guide,* British Standards Institute Std. BS EN 60825-1 (1994).
14 E. Buckley *et al.*, "Multi- viewer autostereoscopic display with dynamically-addressable holographic backlight," *SID Symposium Digest* **39**, 340–344 (2008).
15 Nichia, "Blue laser diode NDHB510APA datasheet." [Online]. Available: http://www.nichia.co.jp/specification/en/product/ld/NDHB510APA-E.pdf.
16 V. Bhatia *et al.*, "High efficiency green lasers for mobile projectors," *Proc. IDW '07* (2007).
17 Opnext, "HL6364DG/65DG datasheet," May 2006. [Online]. Available: http://www.photonic-products.com/products/laserdiodes_visible/opnext/hl6364dg_65dg.pdf.
18 T. Mizushima *et al.*, "A bright and efficient mobile projector using a compact green laser," *SID Symposium Digest* **40**, 268–271 (2009).
19 D. Darmon *et al.*, "Led-illuminated pico projector architectures," *SID Symposium Digest* **39**, 1070–1073 (2008).
20 T. R. M. Sales, "Efficient and uniform illumination with microlens-based band-limited diffusers," *Photonics Spectra* **44**, 49–53 (April 2010).
21 E. R. Méndez *et al.*, "Photofabrication of random achromatic optical diffusers for uniform illumination," *Appl. Opt.* **40**, No. 7, 1098–1108 (2001).
22 D. Lim, "AAXA P1 LCoS-based pico projector review," April 2009. [Online]. Available: http://www.slashgear.com/aaxa-p1-lcos-based-pico-projector-review-2842144/.
23 Syndiant, "SYL2030 overview," June 2010. [Online]. Available: http://www.syndiant.com/products_syl2030.html.
24 Micron, Inc., "MT7DPWV2E datasheet," 2009. [Online]. Available: http://www.displaytech.com/pdf/techdoc/displaytech_WVGA_panel_flyer.pdf.
25 M. J. O'Callaghan *et al.*, "Bistable FLCOS devices for doubled-brightness micro-projectors," *SID Symposium Digest* **40**, 232–235 (2009).
26 M. Handschy, "Moves toward mobile projectors raise issue of panel choice," *Display Devices,* 6–8 (Fall 2007).
27 M. Freeman *et al.*, "Scanned laser pico-projectors: Seeing the big picture (with a small device)," *Opt. Photon. News* **20**, No. 5, 28–34 (2009).

Edward Buckley received his MEng. degree in electrical and electronic engineering from University College London, London, U.K., and his Ph.D. degree from the University of Cambridge, Cambridge, U.K. He is a founder of Light Blue Optics, Inc. (LBO), Colorado Springs, Colarado, and a co-inventor of the revolutionary holographic projection technology upon which the company's products are based. He has authored or co-authored and peer-reviewed over 45 papers and conference proceedings. He is a Senior Member of the Society for Information Display (SID), a senior member of the IEEE, and the recipient of the SID Ben Sturgeon Award in 2009.